Journal of
Microbial & Biochemical Technology

Aminur et al., J Microb Biochem Technol 2017, 9:5
DOI: 10.4172/1948-5948.1000365

Research Article OMICS International

Genome Sequencing Revealed Chromium and Other Heavy Metal Resistance Genes in *E. cloacae* B2-Dha

Aminur R[1,2]*, Björn O[1], Jana J[2], Neelu NN[3], Sibdas G[4] and Abul M[1]

[1]*Systems Biology Research Center, School of Bioscience, University of Skövde, Skövde, Sweden*
[2]*The Life Science Center, School of Science and Technology, Örebro University, SE-701 82 Örebro, Sweden*
[3]*Microbial Diversity Research Centre, Dr. D.Y. Patil Biotechnology and Bioinformatics Institute, Dr. D. Y. Patil Vidyapeeth, Tathawade, Pune-411033, India*
[4]*School of Arts and Science, Iona College, New Rochelle, NY 10801, USA*

Abstract

The previously described chromium resistant bacterium, *Enterobacter cloacae* B2-DHA, was isolated from leather manufacturing tannery landfill in Bangladesh. Here we report the entire genome sequence of this bacterium containing chromium and other heavy metal resistance genes. The genome size and the number of genes, determined by massive parallel sequencing and comparative analysis with other known Enterobacter genomes, are predicted to be 4.22 Mb and 3958, respectively. Nearly 160 of these genes were found to be involved in binding, transport, and catabolism of ions as well as efflux of inorganic and organic compounds. Specifically, the presence of two chromium resistance genes, *chrR* and *chrA* was verified by polymerase chain reaction. The outcome of this research highlights the significance of this bacterium in bioremediation of chromium and other toxic metals from the contaminated sources.

Keywords: Bioremediation; Toxic metals; *Enterobacter cloacae;* Genome sequencing; *De novo* assembly; Gene annotation

Introduction

The global urbanization and industrialization creates increasing levels of pollution including toxic heavy metal contamination [1]. In particular, chromium toxicity is generated through widespread anthropogenic activity via leather processing, steel production, wood preservation, chromium/electroplating, metal processing, alloy formation, textiles, ceramics and thermonuclear weapons manufacturing, and together with agronomic practices such as the use of organic biomass (sewage sludge or fertilizers), which continues to be a major threat to the environment [2-6]. Furthermore, chromium exerts damage directly on human health through toxic and mutagenic effects causing severe DNA damage [7]. However, chromium has multiple effects on bacteria including competitive inhibition of sulphate transport, DNA mutagenesis and protein damage [8]. Microorganisms have developed various mechanisms to survive chromium toxicity: (i) transmembrane efflux of chromate (ii) the ChrR transport system (iii) the reduction of chromate (iv) protection against oxidative stress and (v) DNA repair systems [3,9-15]. In addition, chromate resistance is attributed to the functions of a series of chromosomal or plasmid encoded genes, including the chromium resistance (*chr*) operon comprising of either *chrBAC* or *chrBACF* in bacteria [9,16,17]. The ChrA protein, a member of the CHR superfamily of transporters appears to be active in chromate efflux driven by the membrane potential, whereas the *chrB* gene encodes for a membrane bound protein necessary for the regulation of chromate resistance [18-20]. The *chrC* gene encodes a protein almost similar to iron-containing superoxide dismutase, while the *chrE* gene encodes a protein resembling a rhodanese type enzyme in *Orthrobacterium tritici* 5bvI1 [20]. The *chrF* gene likely encodes a repressor of chromate-dependent induction, whereas the ChrR protein catalyzes one-electron shuttle followed by a two-electron transfer to Cr^{6+} [21].

Previously, we have characterized *E. cloacae* B2-DHA, a soil-borne bacterium, that can survive and grow on medium containing up to 5.5 mM chromate. By using inductively coupled plasma atomic emission spectroscopy (ICP-AES) we have shown that after 120 h of exposure to 100 µg/mL chromium the B2-DHA cells can accumulate 320 µg of chromium per gram dry weight of bacterial biomass thus the concentration of chromium in the cell free growth medium is decreased from 100 µg/mL to 19 µg/mL (81%) [6]. In addition, B2-DHA, can grow on medium containing sodium arsenate, ferric chloride, manganese chloride, zinc chloride, nickel chloride and silver nitrate. However, the mechanisms by which this chromium-adapted B2-DHA survives were not elucidated. Thus, the present study was aimed at demonstrating whether the strain B2-DHA harbored genes that were responsible for chromium and other metal resistance. In this study, we have performed massive parallel genome sequencing of *E. cloacae* B2-DHA to investigate the metal responsive genes. All the genes involved in metal binding activity and reduction of metal by the *E. cloacae* B2-DHA strain were predicted by Rapid Annotations using Subsystems Technology, RAST and/or Blast2GO [22,23]. Furthermore, we have conducted comparative genome analyses of *E. cloacae* B2-DHA with other known *Enterobacter* genome sequences and characterized the genetic rearrangement among the various lineages to understand the evolutionary processes involved in shaping the genomes.

Materials and Methods

Extraction of genomic DNA

Genomic DNA was extracted from *E. cloacae* B2-DHA using DNeasy Blood & Tissue Kit (Qiagen, Cat No 69506) according to manufacturer's instructions with some modifications. The bacteria were cultured in Luria Bertani (LB) medium and pellets were collected from 1.0 ml of bacterial cultures by centrifugation at 8000 rpm for 10 min, the

***Corresponding author:** Aminur R, Department of Molecular Biology, Systems Biology Research Center, School of Bioscience, University of Skövde, Sweden, Tel: +46-500 448679; +46-7389 81928; E-mail: aminur.rahman@his.se

Received August 28, 2017; **Accepted** September 18, 2017; **Published** September 25, 2017

Citation: Aminur R, Björn O, Jana J, Neelu NN, Sibdas G, et al. (2017) Genome Sequencing Revealed Chromium and Other Heavy Me*tal* Resistance Genes in *E. cloacae* B2-Dha. J Microb Biochem Technol 9:191-199. doi: 10.4172/1948-5948.1000365

pellets were resuspended in TE buffer (10 mM Tris- HCl, 1 mM EDTA [pH 8.0]) containing RNase (50 mg/ml) and lysozyme (50 mg/ml) and incubated at 37°C for 2 h instead of using ATL (a tissue lysis buffer). The purity and concentration of the extracted DNA were measured using the Nanodrop® ND-1000 Spectrophotometer (Saveen Werner, USA). The DNA sample exhibiting a clear band in agarose gel electrophoresis was selected for sequencing of the whole genome.

Genome sequencing

The entire genome sequencing of *E. cloacae* B2-DHA was assisted by the Otogenetics Corporation (GA, USA) as follows: (i) Purified 0.5-1.0 µg of genomic DNA sample was clipped into smaller fragments with a Covaris E210 ultrasonicator; (ii) the library of genomic DNA was prepared according to standard protocol of the NEB library preparation kit (New England Biolabs) for the Illumina sequencer with a single sequencing index; (iii) the sequencing was accomplished with the Illumina HiSeq2500 PE106 (106 bp paired-end) read format; (iv) properly paired reads (≥ 30 bp) were separated from the corrected read pool and the remaining singleton reads were combined as single-end reads; and (v) both of the single-end reads and corrected paired-end reads were used in the subsequent *de novo* assembly as described previously [24].

De novo assembly

The *de novo* assembly started with Illumina 106 bp paired-end reads of genomic DNA with an insert length of 300 bp and the read quality was measured with FastQC, version 1.10.1 [25]. Adapter and quality trimming on raw reads were conducted with cutAdapt and K-mer error correction was performed on the adapter-free reads using Quake, version 0.3.5 [26,27]. The paired reads were extracted from the corrected read pool and the remaining singleton reads were listed as single-end reads. Both corrected paired-end and single-end reads were used in the k-mer-based *de novo* assembly. SOAPDenovo, version 2.04 was utilized to perform *de novo* assembly optimization with the error corrected reads [28]. A wide range of K-mers (29-99) were used to identify the scaffold sequences with the largest N50. The optimal scaffold sequences were further subjected to gap closing by utilizing the corrected paired-end reads, and the resulting scaffolds of length ≥ 300 bp were chosen as the final assembly. The largest N50 of 492,970 bp was produced at the k-mer 97. All the scaffolds were ordered by finding the location of the best Blastn hit for each scaffold on the reference genome E. *cloacae* ECNIH2 [NCBI accession number CP008823]. A total of 13 scaffolds were used to order the contigs from a draft genome by comparison to a reference genome performed by following the Mauve Contigs Mover (http://darlinglab.org/mauve/user-guide/reordering.html).

Comparative analysis with other *E-bacter* genomes

The Whole Genome Shotgun project has been deposited at DDBJ/EMBL/GenBank under the GenBank accession LFJA00000000 [29]. The progressive MAUVE algorithm in the MAUVE genome alignment software, version 2.3.1was used to study genome rearrangements in *E. cloacae* B2-DHA and related bacteria. Furthermore, another nucleotide-based dot plot analysis was performed with the Gepard software to (i) compare the 4.21 Mbp chromosomal scaffolds of *E. cloacae* B2-DHA with that of 4.85 Mbp chromosomes in *E. cloacae* ECNIH2, and (ii) investigate the possible genome rearrangements in these strains.

Prediction and annotation of metal responsive genes

The prediction of all genes in B2-DHA genome was carried out using FGenesB and GeneMark. ARAGORN, version 1.2.36 employed to predict tRNA genes in B2-DHA genome. We have applied Blast2GO pipeline using all translated protein coding sequences resulting from the FGenesB to execute all functional annotation analyses. In Blast2GO, the BlastP option was chosen to find the closest homologs in the non-redundant protein databases (nr), followed by employment of Gene Ontology (GO) annotation terms to each gene [30]. An InterPro scan was then performed through the Blast2GO interface with the InterPro IDs for obtaining integrated annotation results [31]. Annotation of all putative metal responsive genes was manually curated. The assembled genome sequence was annotated with RAST which uses (i) the GLIMMER algorithm to predict protein-coding genes (ii) the tRNAscan-SE to predict tRNA genes [32], (iii) an internal script for identification of rRNA genes and (iv)the RNAmmer prediction server version 1.2, to identify rRNA genes [33]. Furthermore, RAST (i) infers putative function(s) of the protein coding genes based on homology with known protein families in phylogenetic neighbor species, and (ii) detects subsystems represented in the genome, and helps to reconstruct the metabolic networks. RAST results obtained in prediction of protein coding genes were compared with the GeneMark and the FGenesB algorithms. Circular plot of ordered contigs of B2-DHA was generated with DNAPlotter to predict the graphical map of the genome [34].

PCR amplification of chromium-responsive genes

Primers for the gene *chrR* and *chrA* were designed by using the Primer3Plus web tool [35]. The two primer pairs, *chrR*-F/*chrR*-R (5'-ATGTCTGATACGTTGAAAGTTGTTA-3'/5'-CAGGCCTTCACCCGCTTA-3') and *chrA*-F/*chrA*-R (5'-TGAAAAGCTGTTTACCCCACT-3'/5'-TTACAGTGAAGGGTAGTCGGTATAA-3') were selected for the detection of *chrR* and *chrA* genes, respectively. PCR amplification of chromium-related marker genes was performed using bacterial genomic DNA as a template in a piko thermal cycler (Finzymes) under the following cycling conditions: 5 min of denaturation at 95°C, followed by 30 cycles of 1 min of denaturation at 95°C, 45 s of annealing at 54.5°C and primer extension at 72°C for 1 min of each Kb product size. All PCR reaction mixtures contained approximately 50 ng DNA templates, 0.2 mM of each deoxyribonucleoside triphosphate, 1X PCR buffer, 0.5 mM of each primer, and 1 U Taq DNA polymerase in a final volume of 50 µl. The final extension reaction was conducted at 72°C for 15 min. PCR products were purified with a QIAquick PCR Purification Kit (Qiagen, Cat No 28104).

Results

Sequencing and de novo genome assembly

Illumina deep sequencing analysis revealed that the genome of B2-DHA consists of 1,756,877,072 bases containing 16,574,312 pairs of reads with an overall GC content of 55%. After quality trimming error correction followed by removal of the TruSeq adaptor sequence, 15,708,650 read pairs (94.78%) and 331,106 single end sequences remained for further analysis. Analysis of the raw reads with FastQC showed that the mean scores per base Phred and per sequence Phred were ≥ 36 and 36, respectively for all positions. The set of scaffold sequences with maximal N50 (492,970 bp) was detected at k-mer 97. The corresponding scaffold sequences were subjected to gap closure using the corrected paired-end reads and the resulting scaffolds (≥ 24300 bp) were defined as the final assembly. The genome summary including the nucleotide content and the gene count is posted in Table 1. The scaffolds were ordered by finding the location of the best Blastn hit for each scaffold on the reference genome *Enterobacter cloacae* ECNIH2. The final assembly of 4,218,945 bp was comprised of 13 scaffolds ranging from 72,208 to 777,700 bp.

Comparative genome analysis

The chromosomal arrangement of *E. cloacae* B2-DHA was compared to *E. cloacae* ECNIH2 by employing progressive Mauve from the Mauve software [36] and Gepard dot plot software [37]. While the alignment remained almost identical in chromosomal rearrangement, the progressive Mauve analysis found several inversions in scaffolds of *E. cloacae* B2-DHA compared to that in *E. cloacae* ECNIH2 (Figure 1A). The dot plot performed with *E. cloacae* B2-DHA and *E. cloacae* ECNIH2 depicted a similar observation of inversions in scaffolds of *E. cloacae* B2-DHA (Figure 1B). Furthermore, several large segments of high similarity were obtained when most parts of the chromosomes of *E. cloacae* B2-DHA and *E. cloacae* ECNIH2 were mapped onto each other (Figure 1B).

AttributeT	Value	% of total
Genome size (bp)	4 218 945	100
DNA GC content (bp)	2 353 515	55
DNA coding region (bp)	3 768779	89,33
Number of replicons	1	
Total scaffolds	13	100
Total genes	4043	100
rRNA genes	22	0,54
tRNA genes	66	1,63
Protein coding genes	3958	97,82
Genes assigned to RAST functional categories	3954	97,79
Genes assigned Gene Ontology terms by Blast2GO	3159	79,87
Largest N50*	492970	
Largest N90*	111054	

Table 1: Summary of the genome of B2-DHA with nucleotide content and gene count.

Gene predictions

The genome and the locations of all genes were predicted through RAST server and the results of this prediction are shown via a circular plot in Figure 2. The prediction of rRNA coding genes showed 22 rRNA genes including four LSU, four SSU, eight 16S and six 23S genes in *E. cloacae* B2-DHA (Figure 2). ARAGORN, version 1.2.36 [38], employed to predict tRNA genes, identified 66 tRNA genes with a GC content ranging from 48.0% to 67.5% in *E. cloacae* B2-DHA.

RAST analysis using the GLIMMER algorithm predicted a total of 3958 protein coding genes of which 3401 could be annotated by RAST's automated homology analysis procedure and assigned to functional categories (Figure 3) [27]. For confirmation of the number of protein coding genes, the FGenesB and the GeneMark algorithms were also applied, yielding 3955 and 3764 genes, respectively [39,40]. By using RAST, we observed that the strain *E. cloacae* B2-DHA contained a large number of genes involved in the ion binding, transport, catabolism and efflux of inorganic as well as organic compounds. More specifically, B2-DHA strain contains many specific metal resistance genes, such

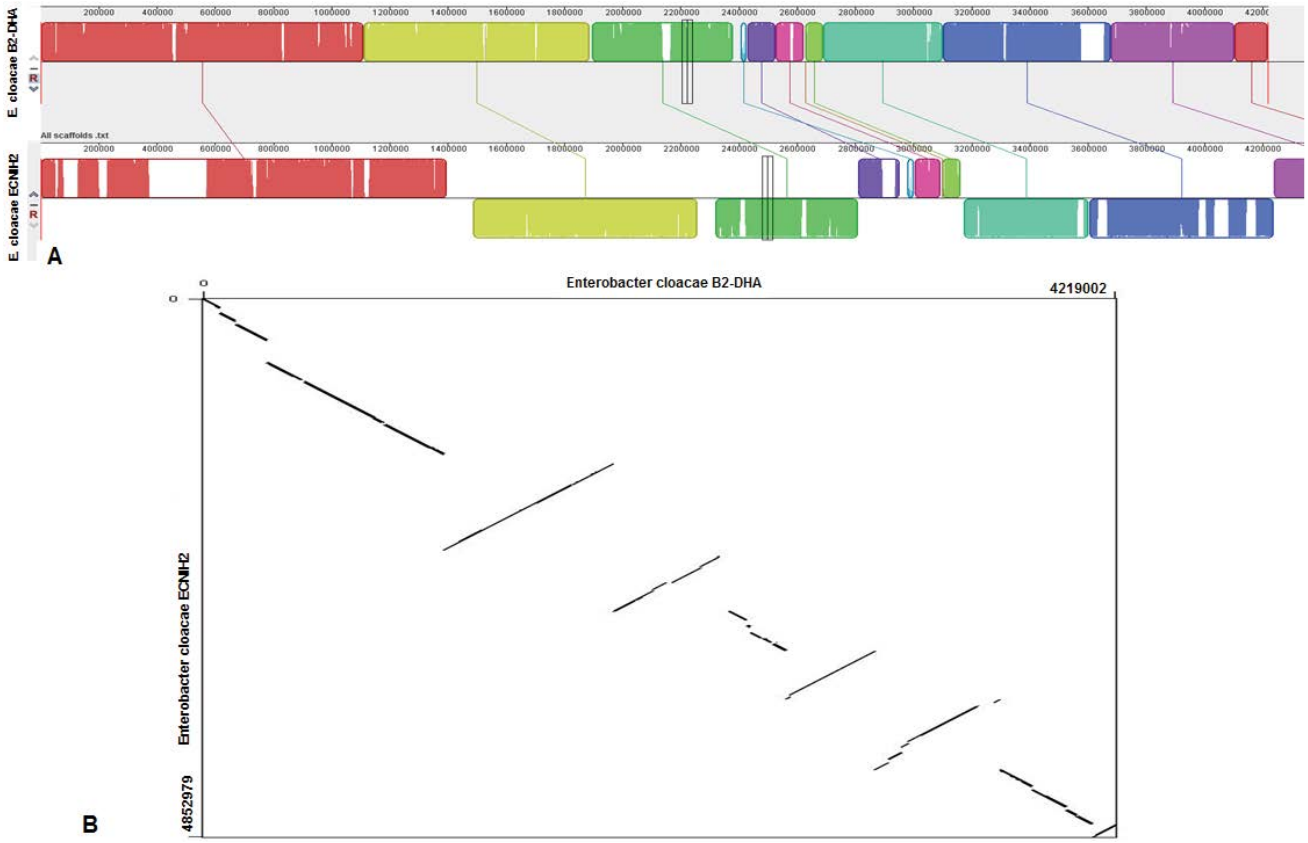

Figure 1: (A) Nucleotide-based alignment of a 4.21 Mbp chromosomal assembly of *E. cloacae* B2-DHA (upper) and 4.85 Mbp chromosomes of *E. cloacae* ECNIH2 (lower). A total of 12 homologous blocks are shown as identically colored regions and linked across the sequences. Regions that are inverted relative to *E. cloacae* B2-DHA are shifted to the right of center axis of the sequence. (B) Dot plot of nucleotide sequences of *E. cloacae* B2-DHA (X-axis) and *E. cloacae* ECNIH2 (Y-axis). Aligned segments are represented as dots, with regions of conservation appearing as lines.

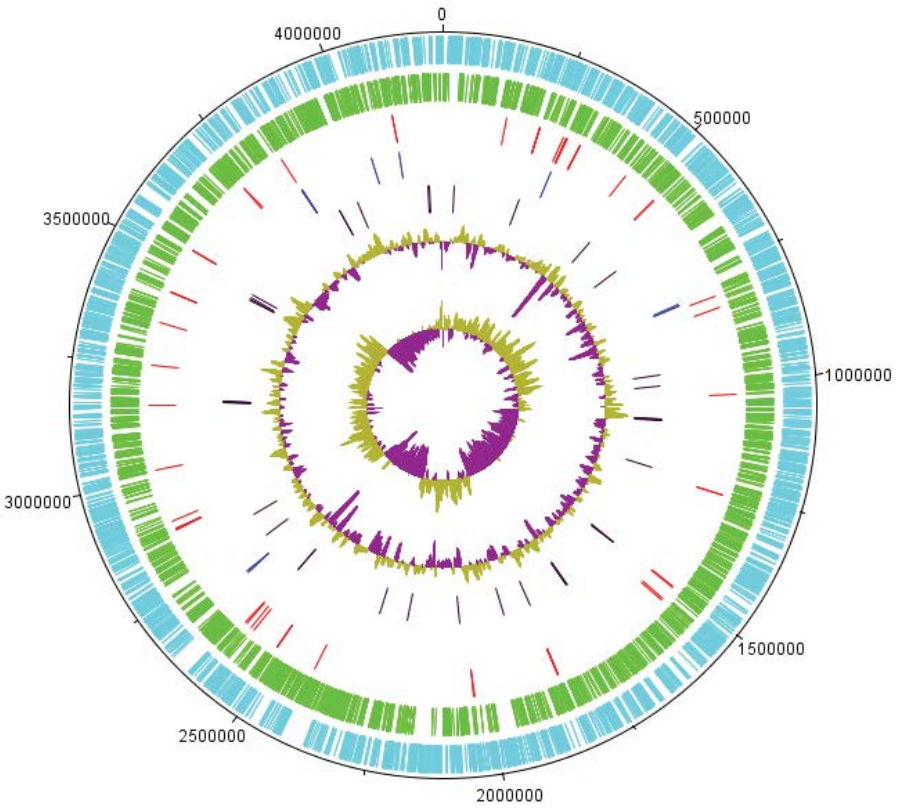

Figure 2: Circular plot of ordered contigs, generated with DNAPlotter. Tracks indicate (from outside inwards) protein coding genes in forward direction (blue) and protein coding genes in reverse direction (green), tRNA genes (red), rRNA genes (dark blue), metal responsive genes (black), GC ratio and GC skew.

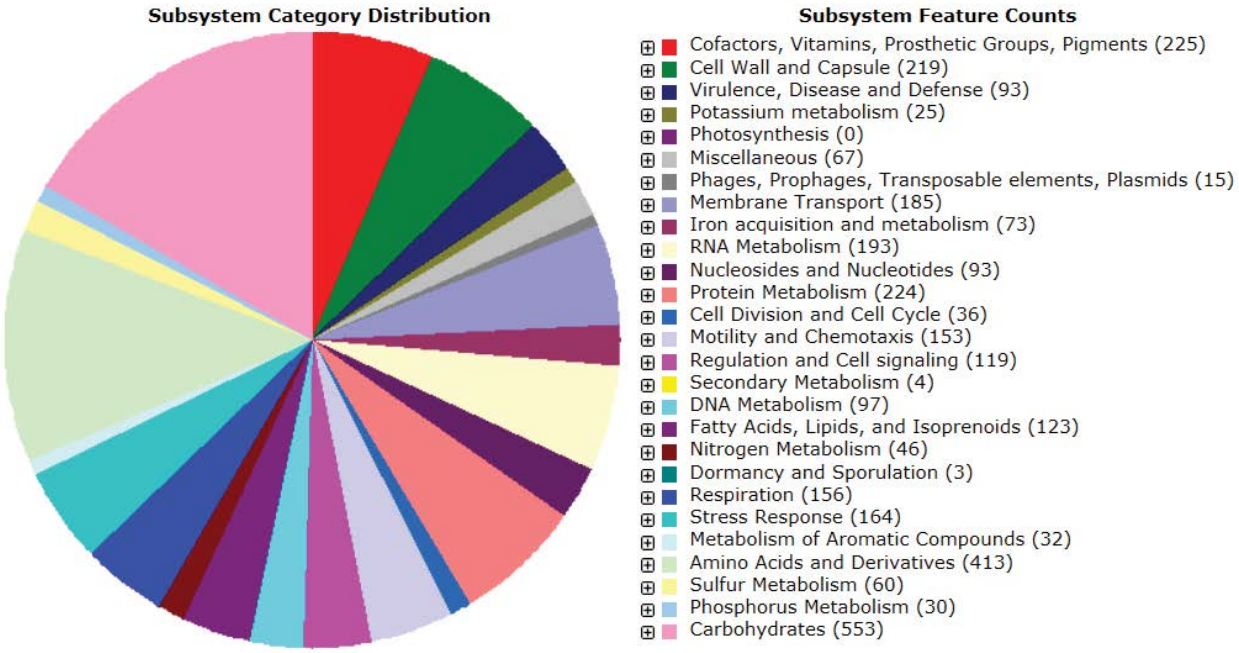

Figure 3: RAST analysis of genes connected to subsystems and their distribution in different functional categories.

as arsenic, chromium, cadmium, cobalt, lead and nickel (Table 2). The Blast2GO pipeline analysis also indicated that B2-DHA contains many genes that are directly responsive to toxic metal ions like arsenic, chromium, cadmium, cobalt, lead and nickel (Table 2). Moreover, these analyses revealed that B2-DHA strain also possesses many genes encoding binding and/or transport of calcium, copper, iron, magnesium, potassium and sodium ions as well as several trace elements like manganese, molybdenum and tellurite (Table 3). Also, a large number of zinc ion binding and/or transporter proteins are retained in this strain (Data not shown). Besides zinc the B2-DHA genome contains a total of 104 proteins involved in binding and transport of other metal ions (Data not shown).

Detection of putative chromium resistance genes

The Blast2GO and RAST analyses detected two chromium reductase genes in B2-DHA. These gene were named as *chrR* and *chrA* (not to be confused with chromate transporter gene). Presence of these genes in this bacterium was verified by PCR amplification (Figure 4). In addition, a number of other chromate responsive genes were confirmed in B2-DHA. Most of these genes have NAD (P) H dependent oxidoreductase activity (Table 4).

Prediction other proteins

Several polymyxin resistant proteins such as PmrM, PmrL, PmrJ and ArnC were aslo predicted by RAST and Blast2GO (Table 4). RAST analysis enabled us to detect several multidrug transporter proteins like MdtA, MdtB, MdtC and MdtD in B2-DHA strain (Table 4). This strain also contains universal stress proteins A, B, C, E and G, as well as several multiple antibiotic resistance proteins such as MarA, MarB, MarC and MarR (Table 4). Other proteins that catalyze binding and transport

			Predicted by	
Start (bp)	**End (bp)**	**Predicted function**	**RAST**	**Blast2GO**
36960	37526	Chromate reductase		X
242454	243404	Magnesium and cobalt transport protein CorA	X	X
495488	496147	ArsR family	X	
615926	616912	Cobalt, zinc, magnesium ion binding		X
964298	965137	Nickel, Cobalt cation transporter activity		X
997848	1000430	Copper, lead, cadmium, zinc, mercury transporting ATPase	X	X
1100748	1099984	Ferric enterobactin transport protein FepC	X	X
1101770	1100781	Ferric enterobactin transport protein FepG	X	X
1102774	1101770	Ferric enterobactin transport protein FepD	X	X
1105147	1104188	Ferric enterobactin transport protein FepB	X	X
1251060	1252157	Chromate reductase	X	X
1510555	1509272	Ferrous iron transport peroxidase EfeB	X	X
1511686	1510559	Ferrous iron transport periplasmic protein EfeO,	X	
1512560	1511727	Ferrous iron transport permease EfeU	X	X
1703726	1704046	Arsenite resistance operon repressor	X	X
1704087	1705376	Arsenite efflux pump protein	X	X
1705389	1705820	Arsenate reductase	X	X
1834407	1835345	Cobalt-zinc-cadmium resistance, Zinc transporter ZitB	X	X
1919484	1921043	Magnesium and cobalt efflux protein CorC	X	
2058555	2059283	Ferric siderophore transport protein TonB	X	
2216754	2216455	Transcriptional regulator, ArsR family	X	
2304506	2303766	Cobalt-zinc-cadmium resistance	X	
2591739	2592824	Cobalt-zinc-cadmium resistance	X	
2592824	2595886	Cobalt-zinc-cadmium resistance protein CzcA	X	
2735411	2736391	Nickel, Cobalt cation transporter activity		X
2810083	2809727	Arsenate reductase	X	X
3168971	3169588	Nickel cation binding		X
3169598	3170242	Nickel cation binding		X
3170821	3171285	Nickel cation binding		X
3171295	3172998	Nickel cation binding		X
3173316	3173618	Nickel cation binding		X
3173629	3174456	Nickel cation binding		X
3170811	3170272	Transport of Nickel and Cobalt, Urea decomposition	X	
3500732	3499869	Nickel incorporation-associated protein HypB	X	X
3505195	3506904	Nickel cation binding		X
3501086	3500736	Nickel incorporation protein HypA	X	X
3516192	3517214	Nickel/cobalt transporter	X	X
3892272	3892499	Ferrous iron transport protein A	X	X
3892530	3894848	Ferrous iron transport protein B	X	
3951655	3953826	Copper, lead, cadmium, zinc, mercury transporting ATPase	X	X
4172744	4173628	Cobalt-zinc-cadmium resistance protein	X	X
4176907	4178211	Arsenic efflux pump protein	X	

Table 2: Heavy metals responsive proteins in B2-DHA predicted by RAST and/or Blast2GO.

Gene	Start	End	Term
Gene 802	858022	859119	manganese ion binding
Gene 196	202800	204344	manganese ion binding
Gene 209	215336	216379	manganese ion binding
Gene 271	277278	279605	molybdenum ion binding
Gene 597	628652	630154	manganese ion binding
Gene 626	664374	665294	manganese ion binding
Gene 720	771440	772036	manganese ion binding
Gene 861	919680	921458	manganese ion binding
Gene 1016	1088133	1089044	Manganese transporter protein SitA
Gene 1017	1089047	1089853	Manganese transporter protein SitB
Gene 1018	1089850	1090701	Manganese transporter protein SitC
Gene 1019	1090695	1091534	Manganese transporter protein SitD
Gene 1049	1125413	1124667	Molybdenum transport protein ModB
Gene 1071	1148010	1150448	molybdenum ion binding
Gene 1223	1294800	1296950	molybdenum ion binding
Gene 1504	1570809	1571876	molybdenum ion binding
Gene 1548	1623197	1625641	molybdenum ion binding
Gene 1610	1694840	1695742	manganese ion binding
Gene 1725	1822796	1821738	Molybdenum transport protein ModC
Gene 1726	1823488	1822796	Molybdenum transport protein ModB
Gene 1727	1824261	1823485	Molybdenum-binding protein ModA
Gene 1729	1824720	1825508	molybdate ion transport
Gene 1756	1853924	1855090	manganese ion binding
Gene 1818	1924327	1924905	manganese ion binding
Gene 1903	2021204	2023633	molybdenum ion binding
Gene 1908	2029753	2033496	molybdenum ion binding
Gene 2091	2224133	2227873	molybdenum ion binding
Gene 2098	2235200	2237611	molybdenum ion binding
Gene 2209	2348836	2349429	Tellurite resistance protein TehB
Gene 2210	2349429	2350424	Tellurite resistance protein TehA
Gene 2610	2758489	2760867	molybdenum ion binding
Gene 2650	2805061	2806479	manganese ion binding
Gene 2682	2845329	2847608	manganese ion binding
Gene 2713	2876204	2877379	Manganese transport protein MntH
Gene 2785	2950966	2953689	molybdenum ion binding
Gene 3085	3280624	3281571	manganese ion binding
Gene 3130	3326886	3328205	manganese ion binding
Gene 3151	3347474	3349207	manganese ion binding
Gene 3540	3756054	3757565	manganese ion binding
Gene 3885	4139417	4141831	molybdenum ion binding
Gene 3886	4141880	4142467	molybdenum ion binding

Table 3: Manganese, molybdenum and tellurite resistant proteins in B2-DHA predicted by RAST and/or Blast2GO.

Seq. Name	Start	End	Predicted function
Gene- 207	213103	213432	Thioredoxin
Gene- 343	355848	356153	Cytochrome-c oxidase activity
Gene- 488	512342	513904	Oxidoreductase activity, reduced flavin or flavoprotein
Gene- 650	692191	693615	Dihydrolipoamide dehydrogenase
Gene- 1057	1135310	1134879	Universal stress protein G
Gene- 1121	1198337	1199287	Universal stress protein E
Gene- 1150	1228221	1230242	NAD(P)H dependent oxidoreductase activity
Gene- 1554	1634190	1635158	Thioredoxin reductase
Gene- 2184	2325505	2324840	Multiple antibiotic resistance protein MarC
Gene- 2185	2325818	2326195	Multiple antibiotic resistance protein MarR
Gene- 2186	2326216	2326596	Multiple antibiotic resistance protein MarA
Gene- 2187	2326629	2326844	Multiple antibiotic resistance protein MarB
Gene- 2364	2487111	2487539	Universal stress protein C
Gene- 2436	2553300	2556080	NADH: flavin oxidoreductase
Gene- 2463	2591265	2590834	Universal stress protein G
Gene- 2531	2669613	2672735	Multidrug resistance MdtB
Gene- 2533	2672736	2675813	Multidrug resistance MdtC
Gene- 2534	2675814	2677229	Multidrug resistance MdtD
Gene- 3334	3544616	3543069	Multidrug resistance MdtB
Gene- 3335	3545805	3544633	Multidrug resistance MdtA
Gene- 3582	3809416	3810390	Quinone oxidoreductase
Gene- 3638	3860171	3862714	Nitrite reductases
Gene- 3746	3974324	3973941	Polymyxin resistance protein PmrM
Gene- 3747	3974644	3974321	Polymyxin resistance protein PmrL,
Gene- 3749	3977186	3976284	Polymyxin resistance protein PmrJ
Gene- 3751	3980145	3979162	Polymyxin resistance protein ArnC
Gene- 3760	3989137	3988850	Universal stress protein B
Gene- 3761	3989469	3989906	Universal stress protein A

Table 4: Universal stress proteins, multiple antibiotic resistant proteins, multidrug resistance proteins and polymyxin resistance protein in B2-DHA as predicted by RAST and/or Blast2GO.

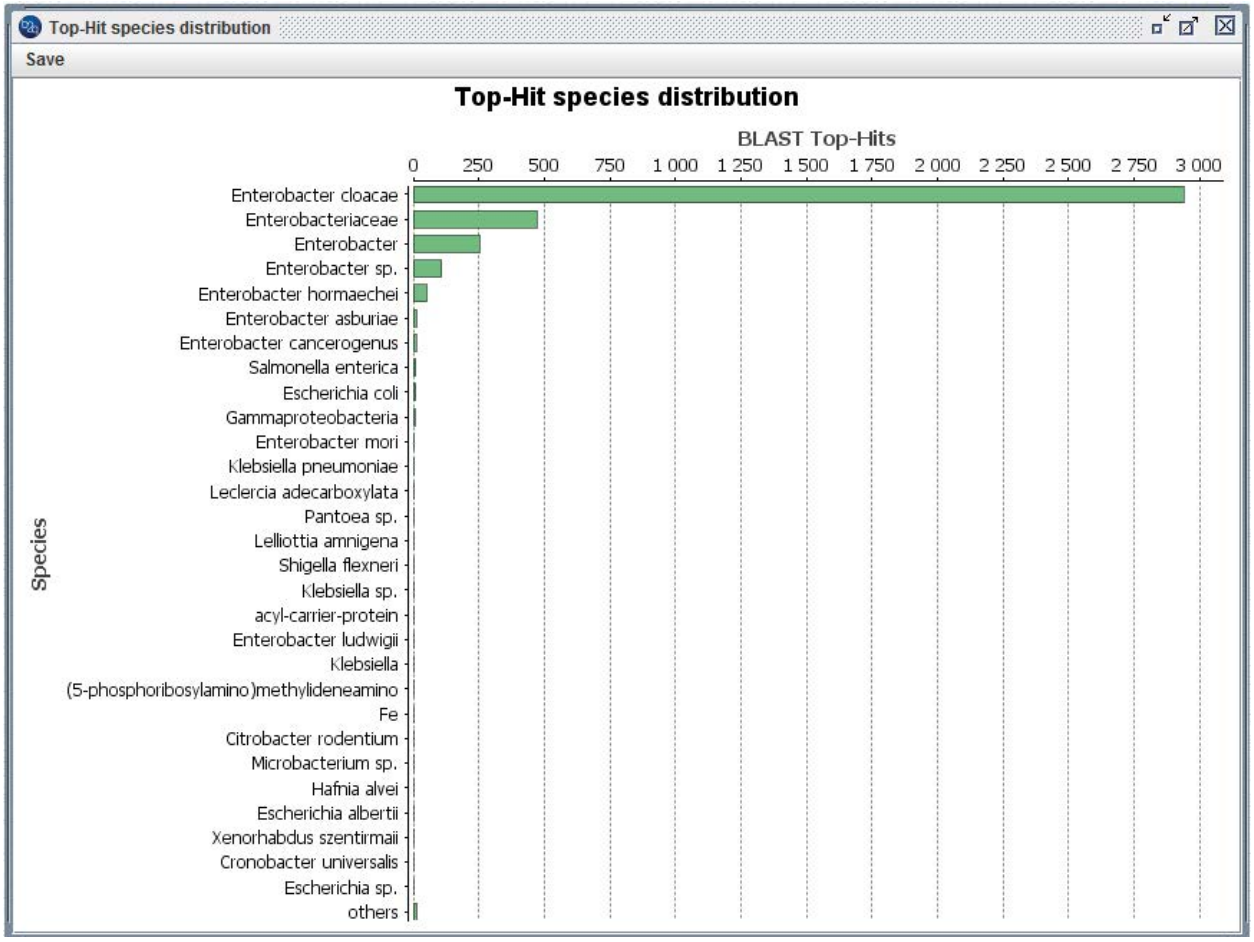

Figure 4: Molecular analysis of chromium responsive genes of B2-DHA and gel electrophoresis. PCR amplification of *chrR* and *chrA* genes. L represents 2 log DNA marker, lane 1 and 2 are the amplified fragments of *chrR* gene in two replicates whereas lane 3 and 4 are the amplified fragments of *chrA* gene in two replicates.

of the metal ions are metalloendopeptidase, metalloexopeptidase, metallopeptidase, metallocarboxypeptidase and metallochaperone. Some metallocenter assembly proteins such as HypA, HypB, HypC, HypD, HypE and HypF are also present in this strain.

Discussion

Previously we have reported chromium-resistant bacterial strain *E. cloacae* B2-DHA isolated from the Hazaribagh tannery areas in Bangladesh [6]. In this paper we report the results of sequencing of the whole-genome of this bacterium. After quality trimming, error correction, and removal of the TruSeq adaptor sequence the genome was *de novo* assembled resulting an approximate genome length of 4.22 Mbp. Several other *Enterobacter* strains have been sequenced previously. For example, *E. cloacae* UW5 had a genome size of 4.9-Mbp and *E. cloacae* ENHKU01 had 4.72-Mbp [41,42]. Our strain *E. cloacae* B2-DHA contained a total of 3958 protein coding genes, whereas in *E. cloacae* ENHKU01 the total number of these genes was 4338. The results we obtained in B2-DHA are in agreement with those reported by other researchers, although the genome size and number of protein coding genes in B2-DHA are slightly smaller than those in *E. cloacae* ENHKU0. The difference in number of protein coding genes in the bacterial strains can be attributed to a common phenomenon. Even in a Gram-positive bacterium, *Lysinibacillus sphaericus* B1-CDA, the number of protein coding genes analyzed by different web tools was found to be different [43,44]. The goal of gene prediction in B2-DHA was to catalogue all the genes encoded within its genome. This prediction facilitates understanding of the mechanisms that might be involved in resistance of this bacterium to chromium and other toxic metals. The annotation of the assembled genome, number of tRNA and rRNA in B2-DHA varied from those found in the reference genome of *E. cloacae* ECNIH2. B2-DHA genome contained 22 rRNA and 66 tRNA genes, whereas in the reference genome ECNIH2 these were 25 and 87, respectively (http://www.ncbi.nlm.nih.gov/nuccore/CP008823). The difference in the number of tRNA genes is a common feature of bacterial and archaeal genomes [45]. These differences could likely be due to the draft status of their B2-DHA genome compared to the reference. However, sometimes annotation systems miss some RNA genes. Furthermore, the bacteria which have the highest number of 16S rRNA genes also have the highest number of tRNA genes [46].

Results obtained from RAST and Blast2GO analyses showed that the bacterium contains many metal resistance genes and there is no significant difference in the obtained results between these two methods (Table 2). Genome sequencing also revealed that B2-DHA harbors many other genes conferring resistance of this bacterium to

polymyxins, multiple drugs and antibiotics. These type genes or their homologues have been identified previously in both Gram-positive and Gram-negative bacteria as well as archaea [47,48]. The proteins encoded by these genes contain many metal-binding residues, which may bind to several metal ions, primarily nickel ions [49,50]. Polymyxin resistance proteins are polycationic antimicrobial peptides that serve as antibiotics for the treatment of infectious diseases caused by multidrug-resistant Gram-negative bacteria. Several bacteria such as *Serratia* sp., *Burkholderia* sp. and *Proteus* sp. are naturally resistant to these antibiotics, whereas other bacteria like *Pseudomonas aeruginosa*, *Acinetobacter baumannii* and *Klebsiella pneumoniae* develop resistance to polymyxins through acquired resistance [51]. The B2-DHA strain contains many metalloproteinase or metalloprotease enzymes. The possible explanation for this is that the bacteria often need to protect themselves from adverse environmental stimuli, including exposure to stress factor, cationic antimicrobial peptides, and toxic metals [52]. To survive in these stress conditions bacteria develop various strategies mainly based on alterations of the lipopolysaccharides (LPSs) in their cell walls, which have overall negative charges and are the initial targets of polymyxins [53]. Other strategies may include efflux pumps and capsule formation [54,55]. Thus, the strain B2-DHA, isolated from highly chromium contaminated tannery industry area may have developed similar mechanisms to survive under adverse conditions.

We also report that B2-DHA contains 219 genes which are responsive to cell wall and capsule development as well as 164 genes which are involved in stress response (Figure 3). Presence of these genes in this bacterium might be accounted for its morphological changes when exposed to chromium. This type of changes is an advantageous trait for this bacterium and it facilitates accumulation of chromium inside the cells [6]. As described in the results, B2-DHA contains a number of chromate reductase genes and most of these have NAD(P)H-dependent oxidoreductase activity (Table 4). Similar kind of results has been reported previously by [56]. B2-DHA also harbors soluble quinone oxidoreductases that are expected to reduce Fe^{3+} and Cr^{6+} and counter oxidative stress [57]. In addition, B2-DHA possesses many other functional genes such as thioredoxin and thioredoxin reductase, dihydrolipoamide dehydrogenase, nitrite reductases, NADH: flavin oxidoreductase, quinones, cytochromes, flavoproteins and proteins with iron sulphur centers (Table 4). These genes are believed to be involved in metal oxidoreductase exhibiting Cr^{6+} reduction as reported previously [58-60]. The proteins encoded by these genes initially catalyze one-electron shuttle followed by a two-electron transfer to Cr^{6+} with the formation of intermediate(s) Cr^{5+} and/or Cr^{4+} before further reduction to Cr^{3+} which is a critical process involved in detoxification of chromium inside the cells [21]. Thus bacteria can survive and grow in a chromium contaminated environment. One of many possible ways to increase the effectiveness of chromium bioremediation by using bacteria is to alter the expression of these genes to minimize oxidative stress during chromate reduction. This approach has been proposed by several other researchers [12,48]. Previously, we have postulated that the B2-DHA is resistant to chromium and it can decrease chromium content significantly in the contaminated source by accumulating it in the cells [6]. Furthermore, we report that the bacterium can reduce Cr^{6+} to Cr^{3+}, corroborating the presence of chromium resistance genes *chrR* and *chrA* as described in this paper.

Conclusion

In this paper we report the genome sequence and annotation of a chromium resistant bacterium, *E. cloacae* B2-DHA. Furthermore, bioinformatics analyses revealed that this bacterium harbours two chromium resistance genes, *chrA* and *chrR* among many metal resistance and other genes. Our previous findings of chromium accumulation and the recent data on genomics and functionality of the genes in B2-DHA (which is under investigation) will provide insights to establish the mechanism of chromium resistance in this strain. Altogether, our findings can be employed in bioremediation of these toxic metals in polluted environments especially industry effluents. In a long-term perspective, millions of people worldwide, in turn, can avoid many lethal diseases caused by chronic exposure of toxic metal poisoning. Therefore, our discoveries have a great potential through further investigations in contributing to a significant positive impact on the socioeconomic status of the people particularly in the developing world.

Acknowledgement

This research was supported by a major grant (AKT-2010-018) from the Swedish International Development Cooperation Agency (SIDA), and partly by a small grant from the Nilsson-Ehle (The Royal Physiographic Society in Lund) foundation in Sweden.

References

1. Rahman A, Nahar N, Nawani NN, Jass J, Desale P, et al. (2014) Isolation of a Lysinibacillus strain B1-CDA showing potentials for arsenic bioremediation. J Environ Sci Health A Tox Hazard Subst Environ Eng 49: 1349-1360.
2. Viti C, Pace A, and Giovannetti L (2003) Characterization of Cr (VI)-resistant bacteria isolated from chromium-contaminated soil by tannery activity. Curr Microbiol 46: 1-5.
3. Chourey K, Thompson MR, Morrell-Falvey J, VerBerkmoes NC, Brown SD, et al. (2006) Global molecular and morphological effects of 24 h chromium(vi) exposure on *Shewanella oneidensis* MR-1. Appl Environ Microbiol 72: 6331-6344.
4. Saha R, Nandi R, Saha B (2011) Sources and toxicity of hexavalent chromium: A review. J Coord Chem 64: 1782-1806.
5. Kamika I, Momba M (2013) Assessing the resistance and bioremediation ability of selected bacterial and protozoan species to heavy metals in metal-rich industrial wastewater. BMC Microbiol 13: 28.
6. Rahman A, Nahar N, Nawani NN, Jass J, Hossain K, et al. (2015a) Bioremediation of hexavalent chromium (VI) by a soil borne bacterium, *Enterobacter cloacae* B2-DHA. J Environ Sci Health A Tox Hazard Subst Environ Eng 50: 1136-1147.
7. Viti C, Marchi E, Decorosi F, Giovannetti L (2014) Molecular mechanisms of Cr(VI) resistance in bacteria and fungi. FEMS Microbiol Rev 38: 633-659.
8. He M, Li X, Guo L, Miller SJ and Rensing C (2010) Characterization and genomic analysis of chromate resistant and reducing *Bacillus cereus* strain SJ1. BMC Microbiol. 10: 1-10.
9. Ramirez-Diaz M, Diaz-Perez C, Vargas E, Riveros-Rosas H, Campos-Garcia J, et al. (2008) Mechanisms of bacterial resistance to chromium compounds. Biometals 21: 321-332.
10. Saier MH (2003) Tracing pathways of transport protein evolution. Mol Microbiol 48: 1145-1156.
11. Cervantes C, Campos-Garcia J (2007) Reduction and efflux of chromate by bacteria. In: Nies, D. H., Silver S. (Eds.). *Molecular Microbiology of Heavy Metals* (ed. Nies DH, Silver S, Springer-Verlag), pp: 407-420.
12. Ackerley DF, Barak Y, Lynch SV, Curtin J, Matin A (2006) Effect of chromate stress on *Escherichia coli* K-12. J Bacteriol 188: 3371-3381.
13. Brown SD, Thompson MR, Verberkmoes NC, Chourey K, Shah M, et al. (2006) Molecular dynamics of the *Shewanella oneidensis* response to chromate stress. Mol Cell Proteomics 5: 1054-1071.
14. Henne KL, Nakatsu CH, Thompson DK, Konopka AE (2009) High-level chromate resistance in *Arthrobacter* sp. strain FB24 requires previously uncharacterized accessory genes. BMC Microbiol 9: 199.
15. Miranda AT, González MV, González EG, Vargas E, Campos-García J, et al. (2005) Involvement of DNA helicases in chromate resistance by *Pseudomonas aeruginosa* PAO1. Mutat Res 578: 202 - 209.

16. Nies A, Nies DH, Silver S (1990) Nucleotide sequence and expression of a plasmid encoded chromate resistance determinant from *Alcaligens eutrophus*. J Biol Chem 265: 5648-5653.

17. Branco R, Chung AP, Johnston T, Gurel V, Morais P, et al. (2008) The chromate-inducible *chrBACF* operon from the transposable element Tn*OtChr* confers resistance to chromium(VI) and superoxide. J Bacteriol 190: 6996-7003.

18. Henson MW, Domingo JWS, Kourtev PS, Jensen RV, Dunn JA, et al. (2015) Metabolic and genomic analysis elucidates strain-level variation in *Microbacterium* spp. isolated from chromate contaminated sediment. Peer J 3: e1395.

19. Pimentel BE, Sa´nchez RM, Cervantes C (2002) Efflux of chromate by *Pseudomonas aeruginosa* cells expressing the ChrA protein. FEMS Microbiol Lett 212: 249-254.

20. Morais PV, Branco R,Francisco R (2011) Chromium resistance strategies and toxicity: What makes *Ochrobactrum tritici* 5bvl1 a strain highly resistant. Biometals 24: 401-410.

21. Cheung KH, Ji-Dong G (2007) Mechanism of hexavalent chromium detoxification by microorganisms and bioremediation application potential: A review. Int Biodeterior Biodegrada 59: 8-15.

22. Aziz RK, Bartels D, Best AA, DeJongh M, Disz T, et al. (2008) The RAST server: Rapid annotations using subsystems technology. BMC Genomics 9: 75.

23. Götz S, García-Gómez JM, Terol J, Williams TD, Nagaraj SH, et al. (2008) High-throughput functional annotation and data mining with the Blast2GO suite. Nucleic Acids Res 36: 3420-3435.

24. Rahman A, Nahar N, Jass J, Olsson B, Mandal A (2016a) Complete genome sequence of *Lysinibacillus sphaericus* B1-CDA, a bacterium that accumulates arsenic. Genome Announc 4: e00999-15.

25. Andrews S (2010) FastQC: A quality control tool for high throughput sequence data.

26. Martin M (2011) Cutadapt removes adapter sequences from high-throughput sequencing reads. EMBnet 17:10-12.

27. Kelley DR, Schatz MC, Salzberg SL (2010) Quake: Quality-aware detection and correction of sequencing errors. Genome Biol 11: R116.

28. Luo R, Liu B, Xie Y, Li Z, Huang W, et al. (2012) SOAPdenovo2: An empirically improved memory-efficient short-read de novo assembler. GigaScience 1: 18.

29. Rahman A, Nahar N, Olsson B, Mandal A (2016b) Complete genome sequence of *Enterobacter cloacae* B2-DHA, a chromium resistant bacterium. Genome Announc 4: e00483-16.

30. Ashburner M, Ball CA, Blake JA, Botstein D, Butler H, et al. (2000) Gene ontology: Tool for the unification of biology. The Gene Ontology Consortium. Nat Genet 25: 25-29.

31. Zdobnov EM, Apweiler R (2001) InterProScan – an integration platform for the signature-recognition methods in InterPro. Bioinformatics 17: 847-848.

32. Lowe TM, Eddy SR (1997) tRNAscan-SE: A program for improved detection of transfer RNA genes in genomic sequence. Nucleic Acids Res 25: 955-964.

33. Lagesen K, Hallin P, Rødland EA, Stærfeldt HH, Rognes T, et al. (2007) RNAmmer: Consistent and rapid annotation of ribosomal RNA genes. Nucleic Acids Res 35: 3100-3108.

34. Carver T, Thomson N, Bleasby A, Berriman M, Parkhill J (2009) DNAPlotter: Circular and linear interactive genome visualization. Bioinformatics (Oxford, England) 25: 119-120.

35. Untergasser A, Nijveen H, Rao X, Bisseling T, Geurts R, (2007) Leunissen: Primer3Plus, an enhanced web interface to Primer3. Nucleic Acids Res 35: W71-W74.

36. Darling AE, Mau B, Perna NT (2010) ProgressiveMauve: Multiple genome alignment with gene gain, loss and rearrangement. PLoS ONE 5: e11147.

37. Krumsiek J, Arnold R, Rattei T (2007) Gepard: A rapid and sensitive tool for creating dot plots on genome scale. Bioinformatics 23:1026-1028.

38. Laslett D, Canback B (2004) ARAGORN, a program to detect tRNA genes and tmRNA genes in nucleotide sequences. Nucleic Acids Res 32: 11-16.

39. Salzberg SL, Delcher AL, Kasif S, White O (1998) Microbial gene identification using interpolated Markov models. Nucleic acids Res 26: 544-548.

40. Salamov AA, Solovyev VV (2000) Ab initio gene finding in Drosophila genomic DNA. Genome Res 10: 516-522.

41. Borodovsky M, Mclninch J (1993) GeneMark: parallel gene recognition for both DNA strands. Comput Chem 17: 123-133.

42. Coulson TJD, Patten CL (2015) Complete genome sequence of *Enterobacter cloacae* UW5, a Rhizobacterium capable of high levels of indole-3-acetic acid production. Genome Announc 3: e00843-15.

43. Liu WY, Wong CF, Chung KMK, Jiang JW, Leung FCC (2013) Comparative genome analysis of *Enterobacter cloacae*. PLoS ONE 8: e74487.

44. Rahman A, Nahar N, Nawani NN, Jass J, Ghosh S, et al. (2015b) Comparative genome analysis of Lysinibacillus B1-CDA, a bacterium that accumulates arsenics. Genomics 106: 384-392.

45. Lee ZMP, Bussema C, Schmidt TM (2009) rrnDB: documenting the number of rRNA and tRNA genes in bacteria and archaea. Nucleic Acids Res 37: D489-D493.

46. Vezzi A, Campanaro S, D'Angelo M, Simonato F, Vitulo N, et al. (2005) Life at depth: *Photobacterium profundum* genome sequence and expression analysis. Science 307: 1459-1461.

47. Paschos A, Bauer A, Zimmermann A, Zehelein E, Böck A (2002) HypF, a carbamoyl phosphate-converting enzyme involved in [NiFe] hydrogenase maturation. J Biol Chem 277: 49945-49951.

48. Rahman A, Nahar N, Nawani NN, Jass J, Ghosh S, et al. (2015c) Data in support of the comparative genome analysis of Lysinibacillus B1-CDA, a bacterium that accumulates arsenics. Data Brief 5: 579-585.

49. Olaitan AO, Morand S, Rolain JM (2014) Mechanisms of polymyxin resistance: Acquired and intrinsic resistance in bacteria. A review article. Front Microbiol 5: 1-18.

50. Moffatt JH, Harper M, Harrison P, Hale JD, Vinogradov E, et al. (2010) Colistin resistance in *Acinetobacter baumannii* is mediated by complete loss of lipopolysaccharide production. Antimicrob Agents Chemother 54: 4971-4977.

51. Campos MA, Vargas MA, Regueiro V, Llompart CM, Alberti S, et al. (2004) Capsule polysaccharide mediates bacterial resistance to antimicrobial peptides. Infect Immun 72: 7107-7114.

52. Padilla E, Llobet E, Domenech-Sanchez A, Martinez-Martinez L, Bengoechea JA, et al. (2010) Klebsiella pneumoniae AcrAB efflux pump contributes to antimicrobial resistance and virulence. Antimicrob Agents Chemother 54: 177-183.

53. Ramírez-Díaz MI, Díaz-Pérez C, Vargas E, Riveros-Rosas H, Campos-García J, et al. (2007) Mechanisms of bacterial resistance to chromium compounds. BioMetals 21: 321-332.

54. McCord JM, Fridovich I (1988) Superoxide dismutase: the first twenty years (1968-1988). Free Radic. Biol Med 5: 363-369.

55. Myers CR, Carstens BP, Antholine WE, Myers JM (2000) Chromium (VI) reductase activity is associated with the cytoplasmic membrane of anaerobically grown *Shewanella putrefaciens* MR-1. J Appl Microbiol 88: 98-106.

56. Viamajala S, Peyton BM, Apel WA, Petersen JN (2002) Chromate/nitrite interactions in *Shewanella oneidensis* MR-1: Evidence for multiple hexavalent chromium [Cr(VI)] reduction mechanisms dependent on physiological growth conditions. Biotechnol Bioeng 78: 770-778.

57. Ackerley DF, Gonzalez CF, Keyhan M, Blake R, Matin A (2004) Mechanism of chromate reduction by the *Escherichia coli* protein, NfsA and the role of different chromate reductases in minimizing oxidative stress during chromate reduction. Environ Microbiol 6: 851-860.

58. Opperman DJ, Van Heerden E (2008) A membrane-associated protein with Cr(VI)-reducing activity from *Thermus scotoductus* SA-01. FEMS Microbiol Lett 280: 210-218.

59. Li X, Krumholz LR (2009) Thioredoxin is involved in U(VI) and Cr(VI) reduction in *Desulfovibrio desulfuricans* G20. J Bacteriol 191: 4924-4933.

60. Bhattacharya P, Barnebey A, Zemla M, Goodwin L, Auer M, et al. (2015) Complete genome sequence of the chromate-reducing bacterium *Thermoanaerobacter thermohydrosulfuricus* strain BSB-33. Standards in Genomic Sciences 10: 74.

This article was originally published in a special issue, **Advances in Microbiology and Biotechnology** handled by Editor(s). Dr. Gamil Sayed Gamil Zeedan, , National Research Center, Egypt